ELSEVIER

Materials Science and Engineering B99 (2003) 588–592

MATERIALS SCIENCE & ENGINEERING B

www.elsevier.com/locate/mseb

Study on the high-pressure properties of KCl crystal by inversion pair potentials

Shuo Zhang [a,*], Nanxian Chen [a,b]

[a] Department of Physics, Tsinghua University, Room 4303, Beijing 100084, People's Republic of China
[b] Institute for Applied Physics, University of Science and Technology Beijing, Beijing 100083, People's Republic of China

Received 10 June 2002; received in revised form 15 August 2002; accepted 10 October 2002

Abstract

Based on the pseudopotential total energies of KCl polymorphism, the new interionic potentials have been derived by lattice inversion techniques. The static properties of B1- and B2-type KCl are calculated to be consistent with the experiments. Then the intermediate states on the B1–B2 transition paths are predicted via the energy minimization at 30 GPa. With the predicted structures, the corresponding band structures and optical properties are also described in terms of the linear muffin-tin orbital atomic-sphere-approximation (LMTO–ASA) method.

Keywords: Interionic potentials; Phase transition; Lattice inversion

PACS numbers: 34.20.Cf; 02.30.Zz; 68.18.JK

1. Introduction

The B1 (NaCl-type) to B2 (CsCl-type) phase transition in alkali chlorides has been attracting much attention for several decades [1–3]. Especially for KCl, the transition pressures for hydrostatic and shock wave transformations are almost equal, [4] so the mechanism about B1–B2 transition has been studied from theoretical and experimental viewpoints [5,6]. In most of the theoretical work [3,7,8], since the first-principle calculations demand much CPU time and memories, the interionic potentials are playing an important role in simulations for B1–B2 phase transition. In previous work, the empirical potentials were often used. However, the empirical potential parameters [7,8] were almost obtained by fitting to the properties of equilibrium state. For the B1–B2 phase transition, the interionic separation and coordination environment are obviously different along the transition path, and the high-pressure induced properties in B2 phase and the B1–B2 transition mechanism could not being totally described by the empirical potentials.

In order to obtain the atomistic pictures about the B1–B2 transition in KCl, based on Chen–Möbius lattice inversion, [9,10] a different method is proposed to derive the new interionic potentials from pseudopotential total-energy curves of KCl polymorphism, which are B1, B2, B3 (zincblende) and one tetragonal structure (T) with $P4/mmm$ symmetry (Fig. 1), respectively. Being valid over a wide range of interionic separations and coordination numbers, this kind of potentials is used to determine the intermediates structures on the pathway connecting the B1 and B2 phases at high pressure. Then the optical properties during the B1–B2 transition can be predicted via the first-principle calculations. Therefore, Section 2 describes the method about how to obtain the interionic pair potentials from the ab initio total-energy curves of KCl polymorphism. Then the intermediate structures between B1 and B2 phases are determined by the inversion potentials in Section 3. The predicted high-pressure optical properties are given from first-principle calculations in Section 4. Finally, conclusions are drawn in Section 5.

* Corresponding author. Tel./fax: +86-106-277-2783.
E-mail address: zhangshuo@mails.tsinghua.edu.cn (S. Zhang).

0921-5107/02/$ - see front matter
doi:10.1016/S0921-5107(02)00543-3

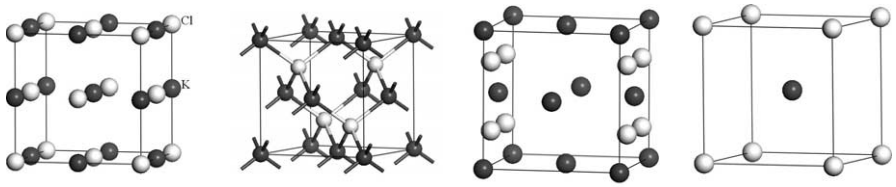

Fig. 1. Structures used to obtain ab initio pseudopotential total energy curve as a function of lattice constant a.

2. Derivation of interionic pair potentials

In order to extract three kind of pair potentials $\phi_{+\,-}$, ϕ_{-} and $\phi_{+\,+}$, we calculated the pseudopotential total-energy curves of KCl in B1, B2, B3 and *P*4/*mmm* structures from lattice constant $a = 4.0$–16.0 Å. These calculations were performed via the CASTEP software package [11,12]. In this paper the ultrasoft pseudopotentials were used and the exchange-correlation energy was taken account by GGA method. The k-mesh points over Brillouin zone were generated with parameters $4 \times 4 \times 4$ for the biggest reciprocal space and $1 \times 1 \times 1$ for the smallest one by Monkhorst–Pack scheme corresponding to the lattice constant. The energy tolerance for SCF convergence is 2×10^{-6} eV per atom. The kinetic energy cutoff for plane wave basis set is 260 eV. The total energy as a function of lattice constant a is shown in Fig. 2.

The interionic pair potential could usually be decomposed into Columbic and non-Columbic terms. In this work, for the Coulombic part, since the electrostatic potential is slowly convergent, the effective charges are determined by fitting to the total-energy difference between B1- and B3-KCl from lattice constant $a =$ 10.0–16.0 Å. With the Madelung constants in B1 and B3 structures, the effective charge q_{eff} is fitted to be 1.005e. For the non-Coulombic contribution, with the identical lattice constant a, the difference between B1 and B3 structures is only about the K^+–Cl^- distance. Then the total-energy difference, $E_{\text{B1}} - E_{\text{B3}}$, between B1 and B3 should only depend on the K^+–Cl^- pair potential and can be written as:

$$E_{\text{B1}} - E_{\text{B3}} = \frac{1}{2}\left[\sum_{\text{B1}} \phi_{+-}(r_{ij}) - \sum_{\text{B3}} \phi_{+-}(r_{ij})\right], \tag{1}$$

where $\phi_{+\,-}$ is the cation–cation pair potential and r_{ij} is the separation between ions i and j ($i \neq j$). Then the $\phi_{+\,-}$ can be inverted from Eq. (1) by Chen–Möbius lattice inversion [9,10].

For the anion–anion potential, since the B1 and T structures have the same K^+ sublattice for lattice constant a, the total-energy difference, $E_{\text{B1}} - E_{\text{T}}$, between B1 and T should be independent on the cation–cation spacing and can be expressed as:

$$E_{\text{B1}} - E_{\text{T}} = \frac{1}{2} \times \left[\sum_{\text{B1}} \phi_{+-}(r_{ij}) + \sum_{\text{B1}} \phi_{--}(r_{ij}) - \sum_{\text{T}} \phi_{+-}(r_{ij}) - \sum_{\text{T}} \phi_{--}(r_{ij})\right]. \tag{2}$$

With the same lattice inversion techniques and above pair potential $\phi_{+\,-}$, the anion–anion pair potential $\phi_{-\,-}$ can be also obtained from Eq. (2).

Since the cation–anion and anion–anion interactions can be calculated for B1, B2, B3 and T structures, the cation–cation pair potential $\phi_{+\,+}$ can also be derived from the total-energy difference between B1- and B2-KCl crystals by lattice inversion method. Based on the final potential curves, the suitable function forms are selected to express the interionic pair potentials as follows:

$$\phi_{++}(r_{ij}) = \frac{q_{\text{eff}}^2}{4\pi\varepsilon_0 r_{ij}}, \tag{3}$$

$$\phi_{--}(r_{ij}) = D_{--}\left\{\exp\left[-\gamma_{--}\left(\frac{r_{ij}}{R_{--}} - 1\right)\right] - 2\exp\left[-\frac{\gamma_{--}}{2}\left(\frac{r_{ij}}{R_{--}} - 1\right)\right]\right\} + \frac{q_{\text{eff}}^2}{4\pi\varepsilon_0 r_{ij}}, \tag{4}$$

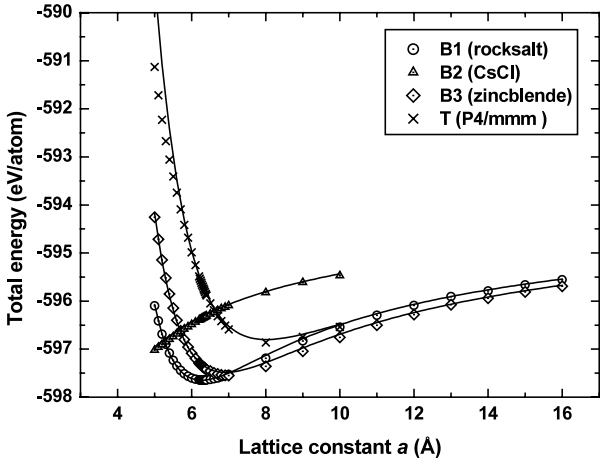

Fig. 2. Calculated pseudopotential total-energy curve as a function of lattice constant a, indicated by different point for KCl polymorphism. The solid lines were calculated by present inversion pair potentials.

$$\phi_{+-}(r_{ij}) = D_{+-}\exp\left[-\gamma_{+-}\left(\frac{r_{ij}}{R_{+-}}-1\right)\right] - \frac{q_{\text{eff}}^2}{4\pi\varepsilon_0 r_{ij}}, \quad (5)$$

in which, the ϕ_{++} is expressed only by Coulomb potential because the corresponding short-range interaction is so small to be neglected. The final potential parameters are listed in Table 1.

3. Determination of high-pressure induced structures

In order to analyze the optical properties of KCl at high pressure, the high-pressure induced structures have to be determined at first, especially the intermediate structures from low-pressure (B1) to high-pressure phases (B2). If these high-pressure structures were all determined from first-principle calculations, the large computational source is demanded. However, once the ab initio interionic potentials are obtained, the high-pressure induced structures can be easily determined by the constant-pressure energy minimization.

In this work, the above inversion pair potentials are firstly used to estimate the transition pressure and calculate the static properties of B1 and B2 phases. The results in Table 2 are in good agreement with the experimental data and previous calculations [13,14], and the transition pressure is predicted to be 2.32 Gpa, close to the experimental value [6]. This indicates that the present pair potentials could be used to predict the high-pressure induced structures for KCl.

Based on the pair potential in Table 1, the 0 °K Gibbs free energy, $F = U_{\text{latt}} + PV$, can be calculated, in which the lattice energy U_{latt} is the sum of all pair potentials, and V is the cell volume at external pressure P. In the present work, the standard cell with eight ions was selected to perform the energy minimization at 30 GPa. In order to obtain the structural parameters of intermediate phases, the motion per relaxation step of each atom was limited within 0.1 Å to search the transformation configurations by steepest descent method. Then the typical configurations from B1 to B2 phase at 30 GPa are shown in Fig. 3.

4. High-pressure band structures and optical properties

Once the structural parameters of intermediate states have been obtained, the high-pressure induced properties could be calculated via the ab initio method. In this work, based on linear muffin-tin orbital atomic-sphere-approximation (LMTO–ASA) method, the electronic structure of KCl was computed by the ESOCS code from MSI [15,16]. The calculated band structures were shown in Fig. 3 to describe the variation of KCl on the high-pressure transition path. From the band structures, it can be seen that the energy gap E_g decrease from B1 ($E_g^{B1} = 7.6$ eV) to B2 ($E_g^{B1} = 5.2$ eV) phase, the value of E_g^{B1} is very close to the experimental result 8.7 eV [17]. On the contrary, the width of valence band extends from 2.3 (experimental value is 2.75 eV [18]) to 7.2 eV. The direct to indirect band transition also occurs during the B1–B2 phase transition in KCl. The most interesting thing is a special energy level appearing in energy gap for P1 intermediate phase. This may be explained by the defects on the B1–B2 path, which introduce the defect energy level between conductive and valence bands. And some experimental evidences [2,6] have supported that the defects play an important role in B1–B2 transition. Therefore, since the intermediate structures seem to be predicted correctly, the corresponding electronic structures could be used to analyze the high-pressure properties in B1–B2 phase transition.

Based on this viewpoint, the optical properties on the path connecting the B1 and B2 phases could be predicted from the above band structures. The results are shown in Fig. 4. For the B1-KCl, a shoulder is found at 1300 Å, and this agrees well the experimental observation [19]. From B1 to B2 state at 30 GPa, the absorption peak at 1300 Å shifts towards the shorter wavelength, and the peak close to the 900 Å shifts to the longer wavelength. After the final B2 phase is achieved, the more absorption peaks appear between 900 and 1300 Å. According to this feature, the absorption spectrum could be used to monitor the phase transition under high pressure.

5. Conclusions

In this work, from the pseudopotential total energies of KCl in B1, B2, B3 and *P*4/*mmm* structures, the new kind of interionic pair potentials is obtained by Chen–Möbius lattice inversion. Since the present potentials can well reproduce the static properties of KCl, the B1–B2 phase transition in KCl were described by energy minimization. The intermediate structures could be determined, and their band structures and optic proper-

Table 1
Interionic pair potential parameters obtained in this work

D_{+-} (eV)	R_{+-} (Å)	γ_{+-}	D_{--} (eV)	R_{--} (Å)	γ_{--}	q_{eff}
1.7149	2.3383	6.4557	0.1177	3.7066	8.8093	1.005 e

The cut-off distance for non-Coulombic short-range potential is 12.0 Å.

Table 2
Calculated static properties of B1- and B2-KCl at zero temperature and pressure

Structure		Lattice constant a_0 (Å)	Bulk modulus B_0 (GPa)	Lattice energy E_{latt} (eV)	Volume at 0 Pa V_0 (Å^3)
B1	This work	6.266	19.12	7.35	61.51
	[14]	6.200	19.35	7.40	62.04
	[13]	6.32	18.6	7.26	63.11
	Experimental [13]	6.294	19.7	7.35	62.33
B2	This work	3.794	23.15	7.25	54.61
	[14]	3.717	26.86	7.30	52.93
	[13]	3.76	–	7.13	–
	Experimental [14]	–	31.6	–	51.87

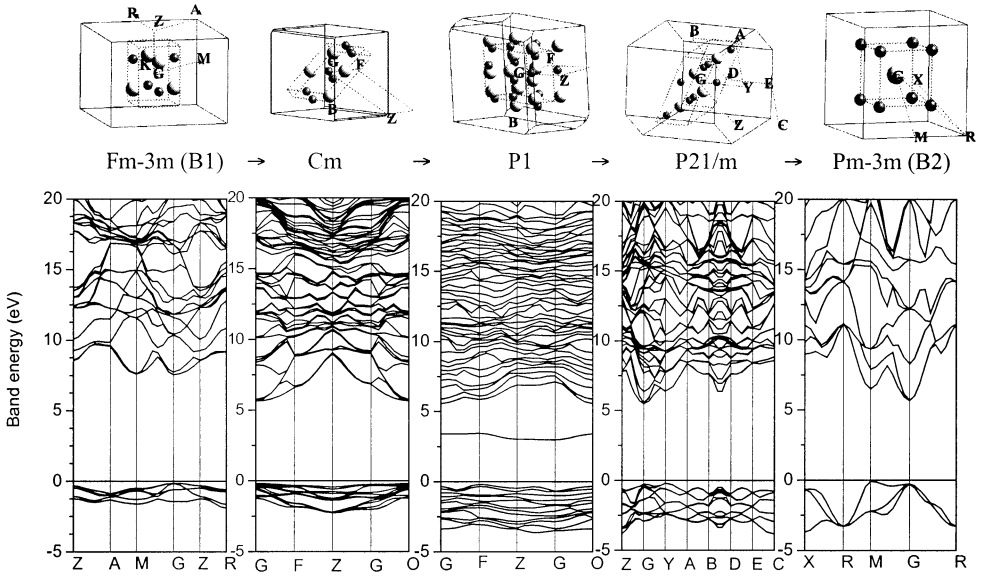

Fig. 3. Intermediate structures and the corresponding band structures on the path of B1–B2 phase transition at 30 GPa.

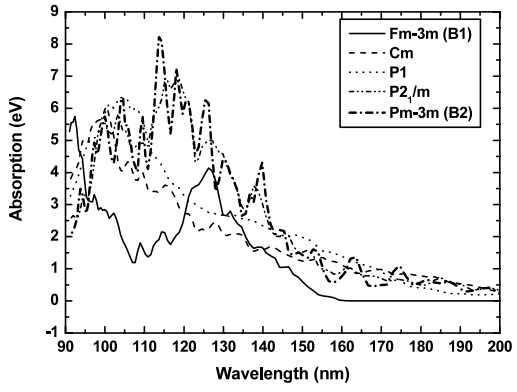

Fig. 4. Calculated absorption spectrums for different states on the path of B1–B2 phase transition for KCl at 30 GPa.

ties were calculated by LMTO–ASA method. According to these predicted properties, it is clear that the high-pressure phase transition could be monitored by the relevant properties. It is worth noting that the effective interionic potentials play an important role in the whole prediction. This may provide a way for atomistic simulation from ab initio calculations to potentials, and then back to ab initio calculations. In this way, the large CPU time for searching the transition states could be effectively saved.

Acknowledgements

This work was supported by the 973 Project in China (Grant No. G2000067101) and National Nature Science Foundation of China (Grant No. 10274035).

References

[1] M. Watanabe, M. Tokonami, N. Morimoto, Acta Crystallogr. Sect. A 33 (1977) 294.
[2] A.R. West, Solid State Chemistry and its Applications, Wiley, New York, 1984.
[3] C.E. Sims, G.D. Barrera, N.L. Allan, Phys. Rev. B 57 (1998) 11164.
[4] G.E. Duvall, R.A. Grapham, Rev. Mod. Phys. 49 (1977) 523.

[5] E.B. Zaretski, G.I. Kanel, P.A. Mogilevski, V.E. Fortov, Sov. Phys. Dokl. 36 (1991) 76.
[6] E. Zaretsky, J. Phys. Chem. Solids 59 (1998) 253.
[7] N. Nakagiri, M. Momura, J. Phys. Soc. Jpn. 51 (1982) 2412.
[8] Y.A. Nga, C.K. Ong, Phys. Rev. B 46 (1992) 10547.
[9] N.-X. Chen, Z.-D. Chen, Y.-C. Wei, Phys. Rev. E 55 (1997) R5.
[10] N.-X. Chen, X.-J. Ge, W.-Q. Zhang, F.-W. Zhu, Phys. Rev. B 57 (1998) 14203.
[11] M.C. Payne, M.P. Teter, D.C. Allan, T.A. Arias, J.D. Joannopoulos, Rev. Mod. Phys. 64 (1992) 1045.
[12] M.D. Segall, P.J.D. Lindan, M.J. Probert, C.J. Pickard, P.J. Hasnip, S.J. Clark, M.C. Payne, J. Phys.: Condens Matter 14 (2002) 2717.
[13] A.J. Cohen, R.G. Gorden, Phys. Rev. B12 (1975) 3228.
[14] H. Zhang, M.S.T. Bukowinski, Phys. Rev. B 44 (1991) 2495.
[15] http://www.accelrys.com/cerius2/cerius246/index.html.
[16] O.K. Andersen, Phys. Rev. B 12 (1975) 3060.
[17] F.C. Brown, C. Gahwiller, H. Fujita, A.B. Kunz, W. Scheifleg, N. Carrera, Phys. Rev. B 2 (1970) 2126.
[18] C.S. Inouye, W. Pong, Phys. Rev. B 15 (1977) 2265.
[19] J.E. Eby, K.J. Teegarden, D.B. Dutton, Phys. Rev. 116 (1959) 1099.